

Conformational adaptations of acyclic receptor templated by weakly coordinating anions

Ivica Đilović,^{a,*} Krunoslav Užarević^{b,c,*}

a) Department of Chemistry, Faculty of Science, University of Zagreb, Horvatovac 102a, 10000 Zagreb (Croatia),
idilovic@chem.pmf.hr

b) Ruđer Bošković Institute, Bijenička 54, 10000 Zagreb, (Croatia), kuzarev@irb.hr

c) Current address: McGill University, Department of Chemistry, 801 Sherbrooke St. West, Montreal, Qc H3A 0B8

General Methods

Chemicals were obtained from Sigma-Aldrich and used without further purification. Solvents and concentrated acids (p.a. grade) were purchased from Kemika, Zagreb.

Preparation of products for analysis

Where needed, the samples were dried in desiccators over CaCl_2 to exclude solvent. The samples for elemental analysis were dried until constant mass.

Infrared Spectroscopy

IR spectra were recorded on a PerkinElmer *Spectrum RXI* FT-IR spectrometer from dried samples dispersed in KBr pellets (4000-400 cm^{-1} range, step 2 cm^{-1}). Dry samples of all complexes were used for data collection, so the bands corresponding to the C–O vibration of methanol could not be observed in any of the spectra.

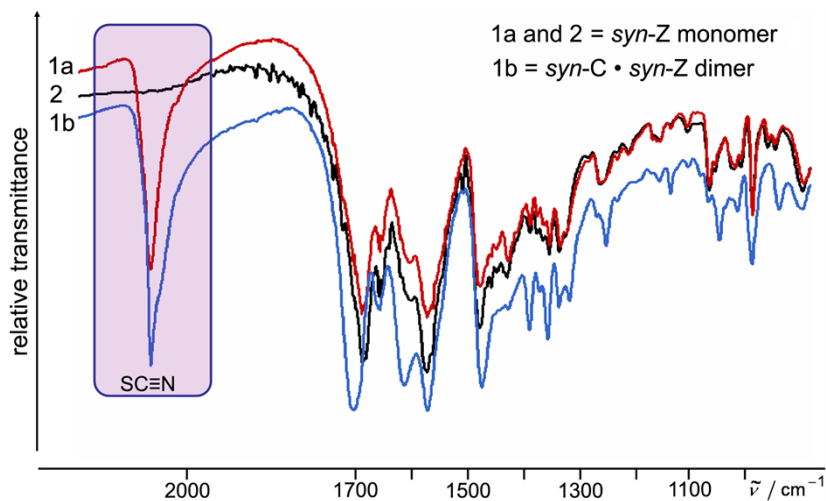


Figure S1. Infrared spectra (1800–900 cm^{-1}) of the dried complexes; **1a** (red), **1b** (blue), and **2** (black).

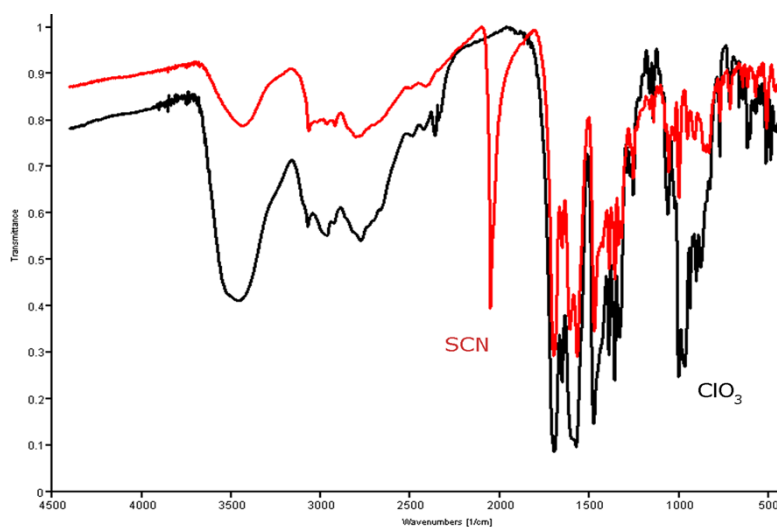


Figure S2. IR spectra (4000–500 cm^{-1}) of complexes **1b** (red) and **3** (black).

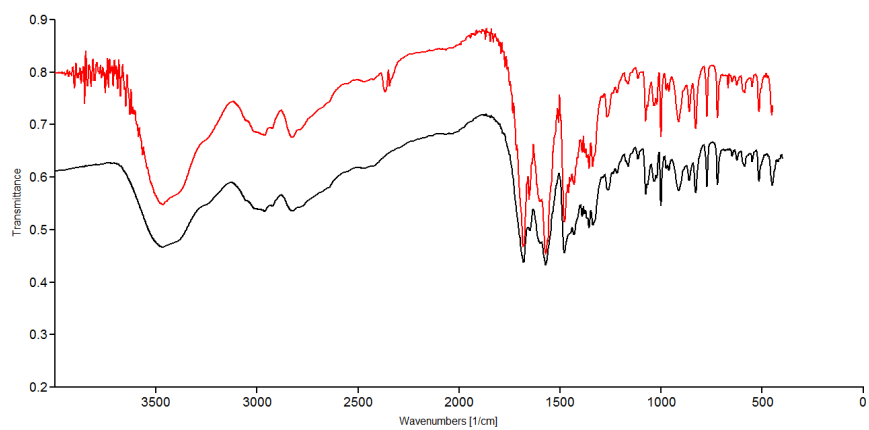


Figure S3. IR spectra (4000–500 cm⁻¹) of iodide (black) and bromide (red) complexes with HL.

X-Ray Crystallography

Single crystals of all compounds, suitable for X-ray crystallography, were obtained from the mother liquid at room temperature. The crystals deteriorate shortly upon exposure to air so the single crystal diffraction data were collected from the crystal mounted in a loop in a mixture of methanol and glycerol, and cooled in nitrogen vapor stream at 100 K. Diffracted intensities were collected on an Oxford Diffraction Xcalibur 3 diffractometer using graphite-monochromated MoK α radiation. The CrysAlis¹ program package was used for data collection, cell refinement and data reduction. The structures were solved by direct methods (SHELXS²). The refinement procedure (SHELXL-97 and 2014³) by full-matrix least squares methods based on F^2 values against all reflections included anisotropic displacement parameters for all non-H atoms. The positions of hydrogen atoms were determined on stereochemical grounds (each riding on their carrier atom). It is worth pointing out that all hydrogen atoms on the positively charged moieties (*viz.* on central nitrogen atoms) were located in the difference Fourier map but were refined using the riding model. In all structures anions are statistically disordered over at least two positions. The SHELX programs operated within the WinGX⁴ suite. A summary of general and crystal data, intensity data collection and structure refinement are presented in Table S1. Molecular graphics were done with PLATON⁵, MERCURY⁶ and ORTEP⁷.

There are two versions of the structure **2**, one with modelled disordered molecules (Figure S9) and the other one in which the electron contribution of the solvent molecules was therefore subtracted from the diffraction data using the PLATON/SQUEEZE²⁴ procedure. The solvent molecules were found to occupy 297 Å³ or 22% of the unit cell. The structure with modelled disorder (CCDC number 1051952), bromide ion was refined in four components and each component was associated with its own free variable. By using the SUMP instruction and its target value, all components were added up to precisely one. Methanol molecule, near to the centre of symmetry was modeled in two positions using negative PART instructions (the site occupancy of each component was set to 0.25).

The X-ray diffraction experiment on the single crystals of iodide complex was conducted several times at low temperature. Nevertheless, the data obtained were not satisfactory and the crystal structure of complex could not be fully refined. The receptor molecule HL and disordered iodide anions molecule were recognized in the Fourier electron density map and refined isotropically (except iodide anions which were refined anisotropically). Unit-cell parameters [$a = 8.1887(4)$ Å, $b = 12.4598(5)$ Å, $c = 13.3536(6)$ Å, $\alpha = 80.017(4)^\circ$, $\beta = 72.510(4)^\circ$, $\gamma = 81.120(4)^\circ$ and $V = 1272.19(10)$ Å³] are comparable to **1a** and **2** suggesting isostructural complexes. Refinement parameters R and wR [$>2\sigma(I)$] are 0.1710 and 0.3819 and for all data 0.1854 and 0.3886, respectively. Goodnes of fit is 1.211 with largest diff. peak and hole (e Å⁻³) of 0.987 and -1.68. Crystal packing is shown in Figure S10.

Supplementary crystallographic data sets for the structures [**1a**, **1b**, **2** (squeezed) and **3**] are available through the Cambridge Structural Data base with deposition numbers CCDC 978263-978265 and 1035947. The second, non-squeezed model of HL:Br⁻ complex is available quoting CCDC number 1051952. Copy of this information may be obtained free of charge from the director, CCDC, 12 Union Road, Cambridge, CB2 1EZ, UK (fax: +44 1223 336 033; e-mail: deposit@ccdc.cam.ac.uk or <http://www.ccdc.cam.ac.uk>).

Table S1. Crystal data and structure refinements parameters for **1a**, **1b**, **2** and **3**

	1a	1b	2	3
Formula	C ₂₂ H ₃₀ N ₄ O ₇ S	C ₂₁ H ₂₆ N ₄ O ₆ S	C ₂₀ H ₂₆ N ₃ O ₆ Br	C ₄₃ H ₆₄ Cl ₂ N ₆ O ₂₁
Crystal size (mm ³)	0.15×0.12×0.10	0.21×0.18×0.15	0.30×0.10×0.03	0.25×0.22×0.13
Space group	<i>P</i> −1	<i>C</i> 2/ <i>c</i>	<i>P</i> −1	<i>P</i> 2 ₁ / <i>n</i>
Temperature (K)	120	150	150	293
Unit cell dimensions				
<i>a</i> (Å)	8.0072(5)	33.554(7)	7.9370(5)	15.9465(6)
<i>b</i> (Å)	11.8432(9)	13.996(3)	12.8236(10)	18.9851(4)
<i>c</i> (Å)	13.3307(9)	18.645(4)	13.4836(10)	17.1610(7)
α (°)	96.449(6)	90.00	79.804(6)	90.00
β (°)	106.07(6)	100.54(3)	76.806(6)	111.55(1)
γ (°)	97.869(6)	90.00	78.841(6)	90.00
Volume (Å ³)	1188.2(1)	8608(3)	1298.1(1)	4862.2(3)
<i>Z</i>	2	16	2	4
<i>D</i> _{calc} (g cm ^{−3})	1.382	1.428	1.249	1.473
μ (mm ^{−1})	0.187	0.198	1.669	0.223
<i>F</i> (000)	524	3904	478	2264
Refl. collected/independent	8861/4543	20162/8419	10549/2847	54110/8464
No. observed refl. [<i>I</i> >2 σ (<i>I</i>)]*	2443	4099	1566	6653
No. restraints/No. parameters	0/309	0/595	0/275	6/668
<i>R</i> / <i>wR</i> [<i>I</i> >2 σ (<i>I</i>)]*	0.0732/0.1353	0.0481/0.0749	0.1041/0.3058	0.0665/0.1859
<i>R</i> / <i>wR</i> [all data]	0.1560/0.1589	0.0872/0.1291	0.1452/0.3386	0.0816/0.1971
Goodness-of-fit on <i>F</i> ²	0.970	0.841	1.161	1.033
Largest diff. peak and hole (e Å ^{−3})	0.639, −0.387	0.297, −0.322	1.146, −0.902	1.192, −0.538

* $R = \sum ||F_o| - |F_c|| / \sum F_o$, $w = 1/[\sigma^2(F_o^2) + (g_1P)^2 + g_2P]$ where $P = (F_o^2 + 2F_c^2)/3$; $S = \sum [w(F_o^2 - F_c^2)^2 / (N_{obs} - N_{param})]^{1/2}$.

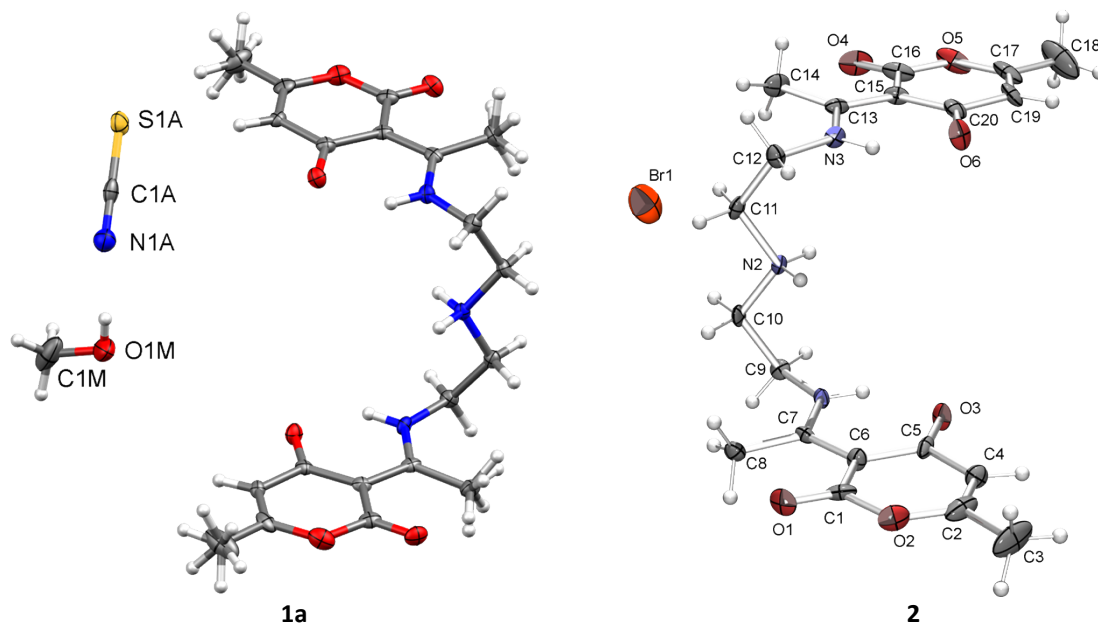
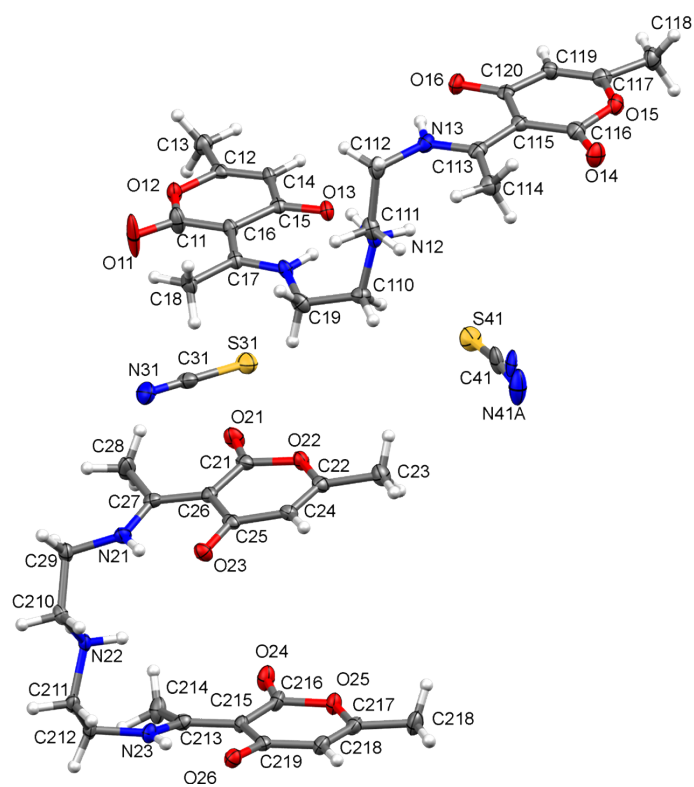
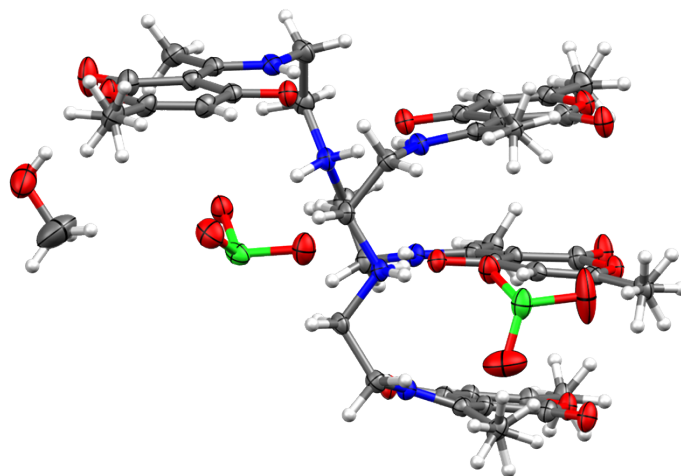


Figure S4. ORTEP-POV-Ray rendered view of the molecular structure of HL⁺ in **1a** and **2**. Displacement ellipsoids are drawn at the 50% probability level. Hydrogen atoms are presented as spheres of arbitrary small radii. Atom color scheme: carbon grey; hydrogen white; nitrogen blue; oxygen red. Hydrogen bonds are drawn as an array of yellow cylinders.

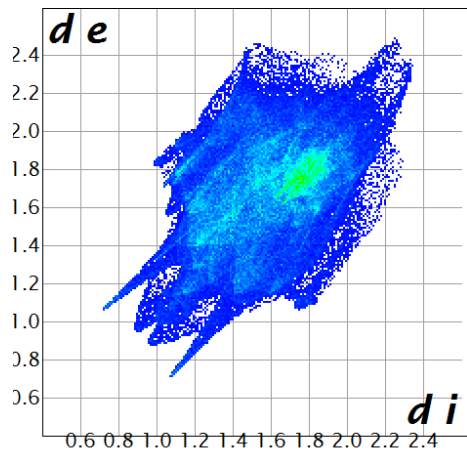


1b

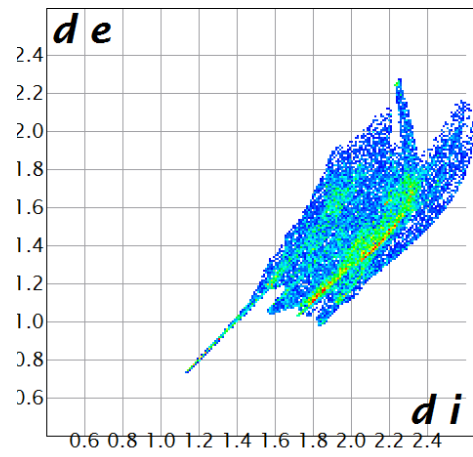


3

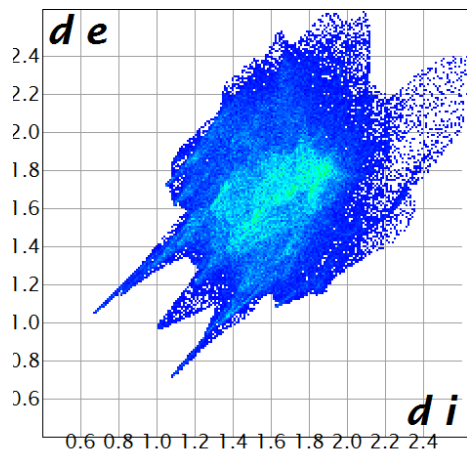
Figure S5. ORTEP-Pov-Ray rendered view of the molecular structure of HL⁺ in **1b** and **3**. Displacement ellipsoids are drawn at the 50% probability level.



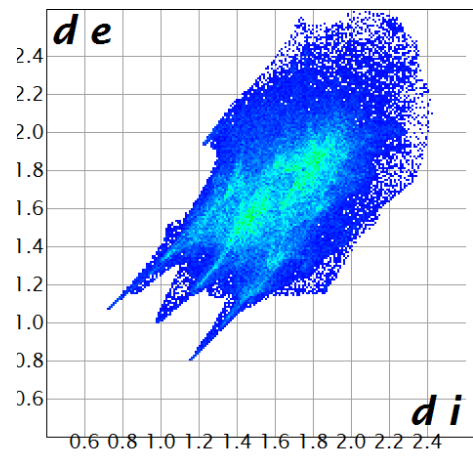
Z-conformer in **1a**



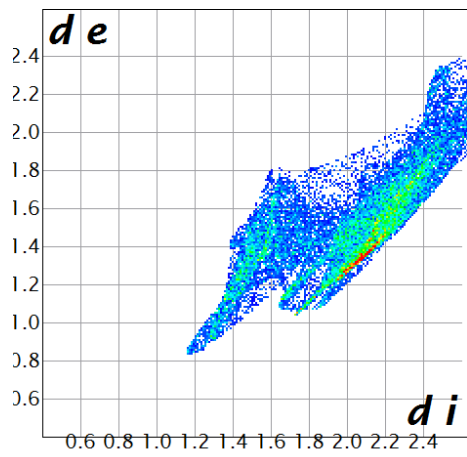
SCN⁻ in **1a**



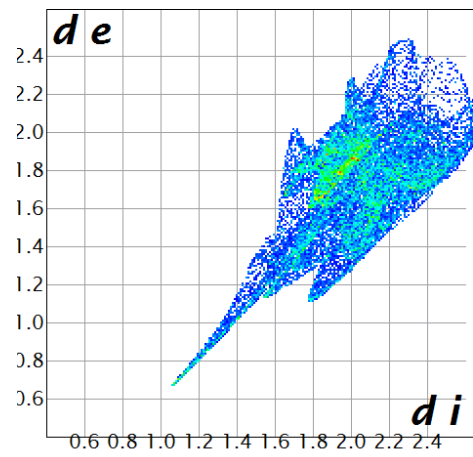
Z-conformer in **1b**



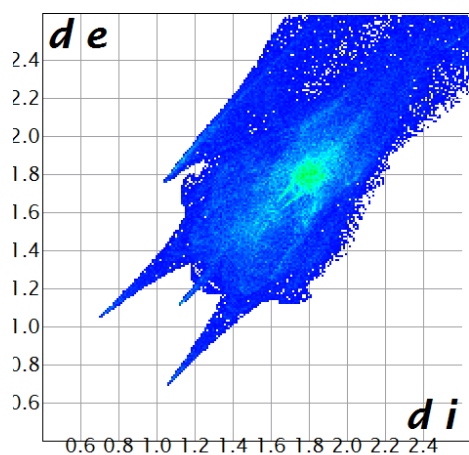
C-conformer in **1a**



disordered SCN⁻ in **2**

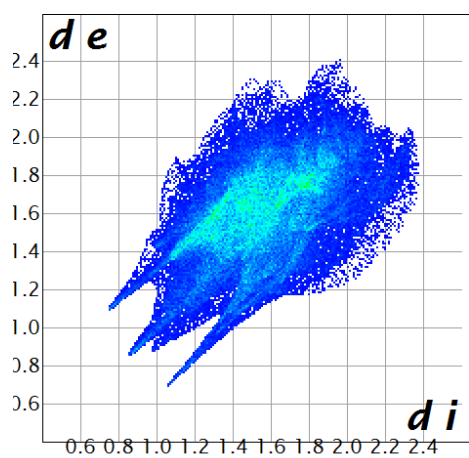


SCN⁻ in **2**

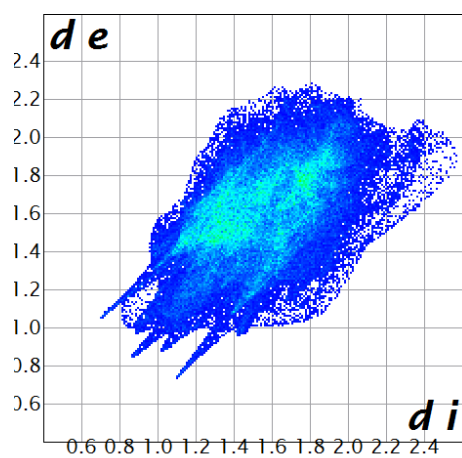


Z-conformer in 2

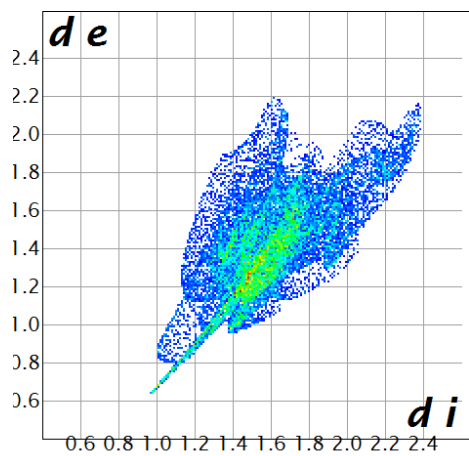
anion finger plot is not generated due to disorder



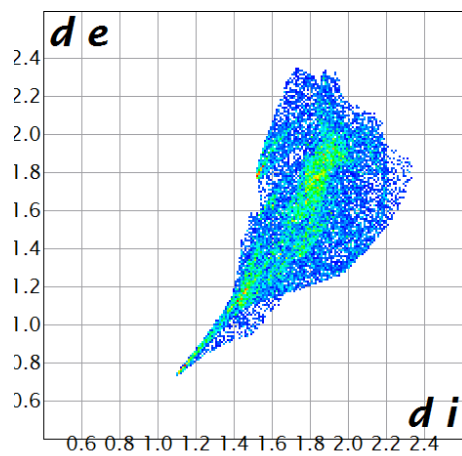
Z-conformer in 3



C-conformer in 3



disordered ClO_3^- in 3



ClO_3^- in 3

Figure S6. Two-dimensional fingerprint plots derived from Hirshfeld surfaces.^[8]

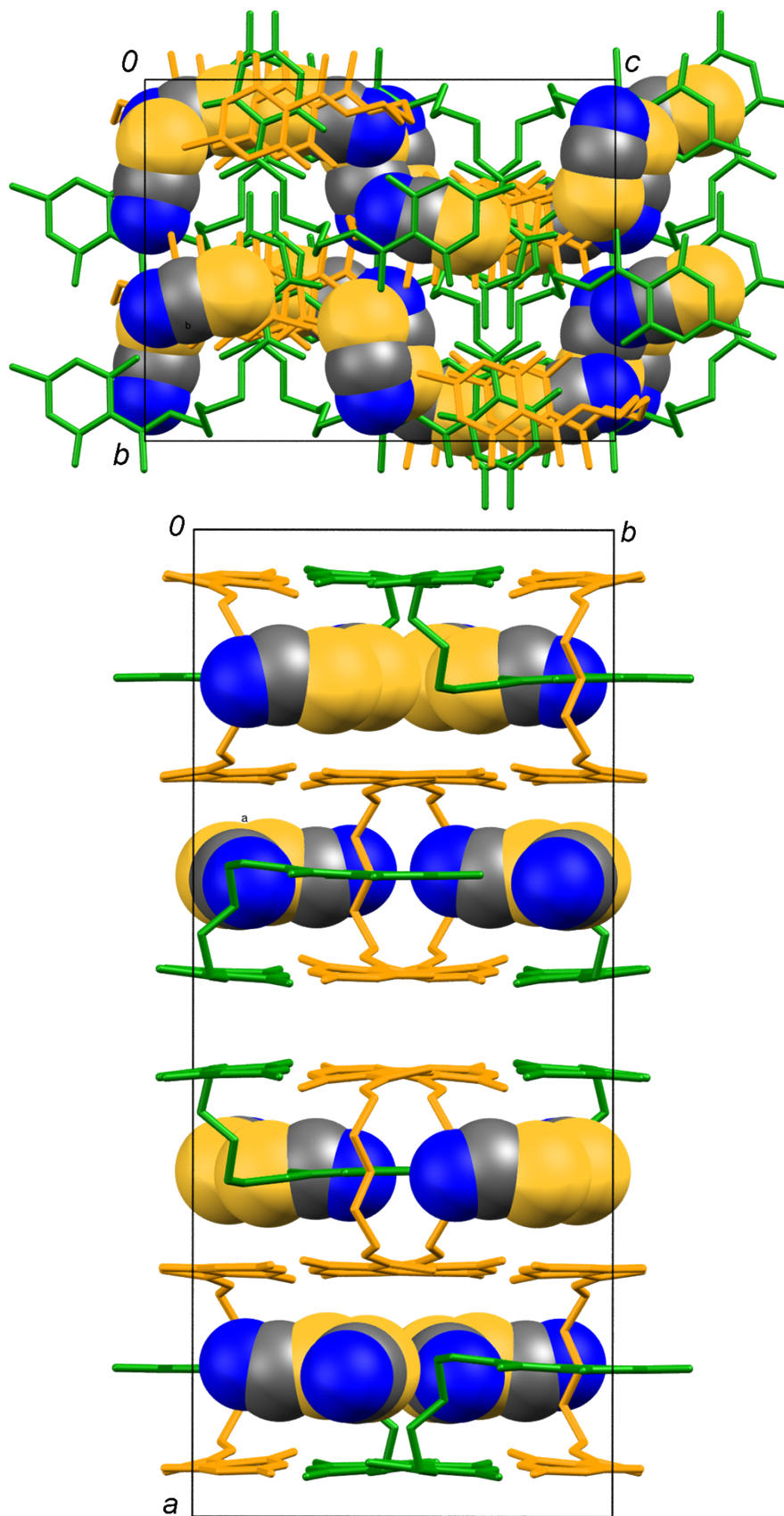


Figure S7. Crystal packing of **1b** viewed down crystallographic *a*- (up) and *c*- axis (down).

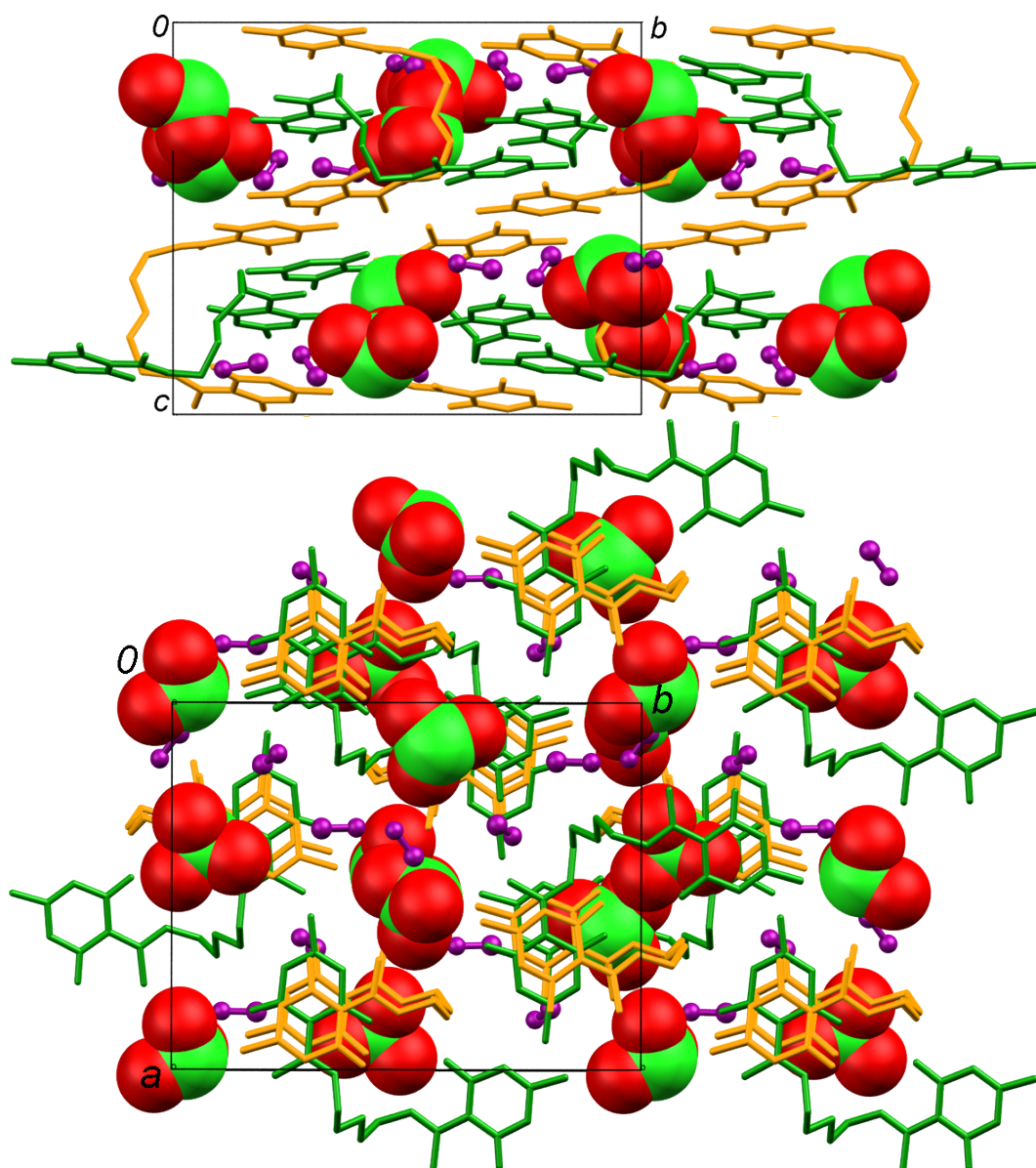


Figure S8. Crystal packing of **3** viewed down crystallographic a - (up) and c - axis (down).

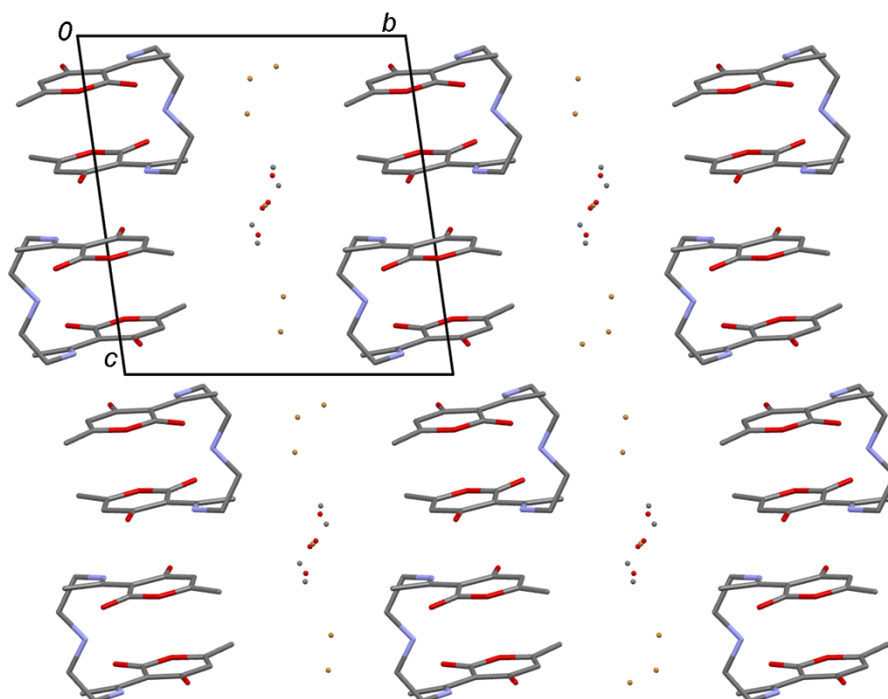


Figure S9. Crystal packing of **2** (non-squeezed model) viewed down crystallographic a -axis. Disordered methanol molecules and bromide ions are located in channels parallel to the crystallographic ac -plane (shown as spheres).

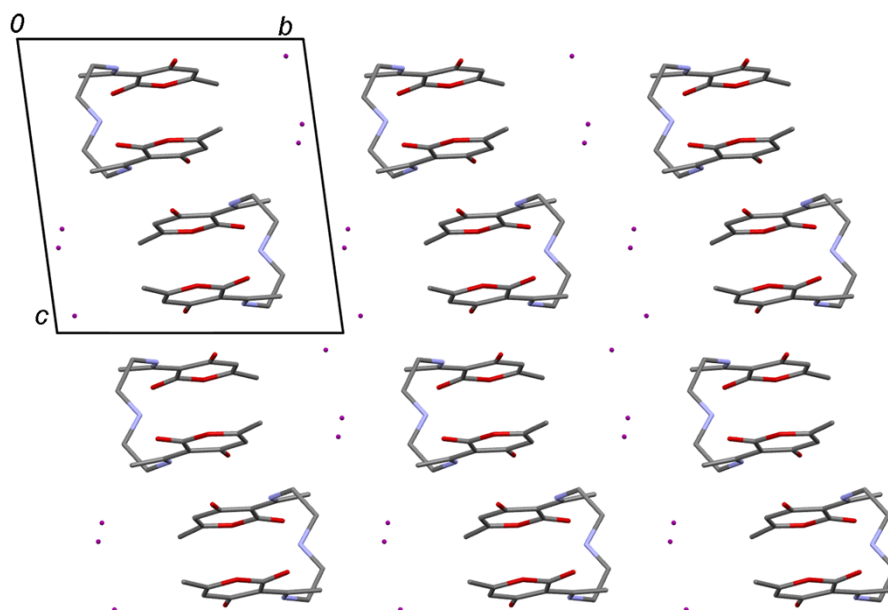


Figure S10. Crystal packing of HL:I⁻ complex viewed down crystallographic a -axis.

Table S2. Selected bond lengths (Å) for **1a**.

S1A–C1A	1.638(4)	N1A–C1A	1.172(6)
O1–C1	1.227(6)	O1M–C1M	1.481(7)
O2–C1	1.378(6)	O1M–H1M	0.840
O2–C2	1.383(6)	C1–C6	1.434(5)
O3–C5	1.252(4)	C2–C4	1.334(5)
O4–C16	1.231(6)	C2–C3	1.482(7)
O5–C16	1.375(6)	C4–C5	1.423(5)
O5–C17	1.374(6)	C5–C6	1.444(6)
O6–C20	1.256(4)	C6–C7	1.430(6)
N1–C9	1.465(5)	C7–C8	1.499(7)
N1–C7	1.315(4)	C9–C10	1.515(5)
N2–C11	1.492(5)	C11–C12	1.527(6)
N2–C10	1.494(5)	C13–C14	1.492(7)
N3–C12	1.467(5)	C13–C15	1.432(6)
N3–C13	1.321(5)	C15–C16	1.434(5)
N1–H1	0.880	C15–C20	1.440(6)
N2–H2B	0.920	C17–C19	1.337(5)
N2–H2A	0.920	C17–C18	1.475(6)
N3–H3	0.880	C19–C20	1.442(6)

Table S3. Hydrogen bonding geometry (Å, °) for **1a**.

	$d(\text{D–H})/\text{Å}$	$d(\text{H}\cdots\text{A})/\text{Å}$	$d(\text{D}\cdots\text{A})/\text{Å}$	$\eta(\text{D–H}\cdots\text{A})/^\circ$	symmetry operator
N1–H1 \cdots O3	0.880	1.860	2.583(4)	139.0	.
N1–H1 \cdots O3	0.880	2.590	3.042(4)	113.0	1–x, 1–y, 1–z
O1M–H1M \cdots N1A	0.840	2.000	2.837(5)	172.0	.
N2–H2A \cdots O1	0.920	1.860	2.715(4)	154.0	–1+x, y, z
N2–H2B \cdots O4	0.920	1.850	2.698(4)	152.0	1+x, y, z
N3–H3 \cdots O6	0.880	1.850	2.581(4)	140.0	.
C8–H8C \cdots O1	0.980	2.340	2.738(5)	103.0	.
C8–H8D \cdots O1	0.980	1.960	2.738(5)	135.0	.
C9–H9A \cdots O3	0.990	2.550	3.145(4)	118.0	1–x, 1–y, 1–z
C9–H9B \cdots O1M	0.990	2.400	3.387(5)	177.0	1–x, 1–y, 1–z
C12–H12A \cdots O6	0.990	2.540	3.176(5)	122.0	1–x, 1–y, 2–z
C14–H14C \cdots O4	0.980	2.330	2.726(5)	103.0	.
C14–H14D \cdots O4	0.980	1.950	2.726(5)	134.0	.
C19–H19 \cdots S1A	0.950	2.850	3.784(4)	167.0	.

Table S4. Selected bond lengths (Å) for **1b**.

O15–C116	1.402(3)	C25–C26	1.441(4)
O16–C120	1.258(3)	N22–H22A	0.900
O21–C21	1.206(4)	N23–H23	0.860
O22–C22	1.362(3)	N41A–C41	1.169(19)
O22–C21	1.396(3)	N41B–C41	1.21(2)
O23–C25	1.262(3)	N31–C31	1.167(4)
O24–C216	1.204(4)	C11–C16	1.428(4)
O25–C216	1.400(3)	C12–C13	1.477(4)
O25–C217	1.365(3)	C12–C14	1.323(4)
O26–C220	1.270(3)	C14–C15	1.425(4)
N11–C19	1.449(4)	C15–C16	1.450(4)
N11–C17	1.317(3)	C16–C17	1.418(4)
N12–C111	1.479(3)	C17–C18	1.500(4)
N12–C110	1.489(3)	C19–C110	1.491(4)
N13–C112	1.459(3)	C111–C112	1.512(4)
N13–C113	1.321(3)	C113–C114	1.482(4)
N11–H11	0.860	C113–C115	1.431(4)
N12–H12B	0.900	C26–C27	1.430(4)
N12–H12A	0.900	C27–C28	1.481(4)
N13–H13	0.860	C29–C210	1.514(4)
C115–C116	1.435(4)	C211–C212	1.504(4)
C115–C120	1.446(4)	C213–C214	1.486(4)
C117–C118	1.489(4)	C213–C215	1.440(4)
C117–C119	1.323(4)	C215–C220	1.431(4)
C119–C120	1.433(4)	C215–C216	1.435(4)
C21–C26	1.449(4)	C217–C219	1.322(4)
C22–C23	1.486(4)	C217–C218	1.479(4)
C22–C24	1.323(4)	C219–C220	1.425(4)
C24–C25	1.436(4)		

Table S5. Hydrogen bonding geometry (Å, °) for **1b**.

	$d(\text{D-H})/\text{Å}$	$d(\text{H}\cdots\text{A})/\text{Å}$	$d(\text{D}\cdots\text{A})/\text{Å}$	$\eta(\text{D-H}\cdots\text{A})/\text{°}$	symmetry operator
N11-H11 \cdots O13	0.860	1.810	2.551(3)	143.0	.
N12-H12A \cdots N31	0.900	1.820	2.688(3)	161.0	$x, 1-y, 1/2+z$
N12-H12B \cdots N11	0.900	2.490	2.901(3)	108.0	.
N12-H12B \cdots O26	0.900	2.040	2.881(3)	154.0	$1/2-x, 1/2+y, 1/2-z$
N13-H13 \cdots O16	0.860	1.820	2.549(3)	142.0	.
N21-H21 \cdots O23	0.860	1.820	2.557(3)	143.0	.
N22-H22A \cdots O13	0.900	1.900	2.792(3)	171.0	$1/2-x, -1/2+y, 1/2-z$
N22-H22B \cdots N41A	0.900	2.080	2.914(15)	153.0	6_555
N22-H22B \cdots O11	0.900	2.250	2.889(3)	127.0	$1/2-x, 3/2-y, -z$
N23-H23 \cdots O26	0.860	1.830	2.567(3)	143.0	.
C111-H11C \cdots O15	0.970	2.450	3.278(3)	143.0	$x, 1-y, -1/2+z$
C111-H11D \cdots S41	0.970	2.850	3.771(3)	160.0	.
C112-H11E \cdots O26	0.970	2.540	3.149(3)	121.0	$1/2-x, 1/2+y, 1/2-z$
C114-H11I \cdots O14	0.960	2.410	2.739(3)	10.0	.
C118-H11K \cdots O24	0.960	2.400	3.315(4)	160.0	$1/2-x, 3/2-y, 1-z$
C14-H14 \cdots N41A	0.930	2.340	3.26(2)	171.0	$x, 1+y, z$
C18-H18B \cdots O11	0.960	2.060	2.814(4)	134.0	.
C210-H21A \cdots O23	0.970	2.580	3.146(3)	118.0	$1/2-x, 1/2-y, -z$
C210-H21B \cdots O12	0.970	2.470	3.320(3)	146.0	$1/2-x, 3/2-y, -z$
C211-H21D \cdots O12	0.970	2.400	3.267(3)	148.0	$1/2-x, 3/2-y, -z$
C214-H21I \cdots O24	0.960	2.350	2.779(3)	107.0	.
C24-H24 \cdots O21	0.930	2.480	3.346(3)	155.0	$1/2-x, -1/2+y, 1/2-z$
C28-H28B \cdots O21	0.960	2.340	2.749(3)	105.0	.
C219-H219 \cdots O14	0.930	2.440	3.326(4)	160.0	$1/2-x, 1/2-y, 1-z$

Table S6. Selected bond lengths (Å) for **2**.

O1–C1	1.224(9)	N3–H3	0.880
O2–C1	1.372(9)	C1–C6	1.415(10)
O2–C2	1.365(9)	C2–C3	1.514(13)
O3–C5	1.247(9)	C2–C4	1.320(11)
O4–C16	1.201(10)	C4–C5	1.456(10)
O5–C16	1.366(10)	C5–C6	1.459(9)
O5–C17	1.369(11)	C6–C7	1.440(9)
O6–C20	1.266(9)	C7–C8	1.478(9)
N1–C7	1.329(9)	C9–C10	1.543(9)
N1–C9	1.432(8)	C11–C12	1.514(9)
N2–C10	1.492(8)	C13–C14	1.485(10)
N2–C11	1.519(8)	C15–C16	1.453(10)
N3–C12	1.468(8)	C15–C20	1.437(10)
N3–C13	1.325(8)	C17–C19	1.326(11)
N1–H1	0.880	C17–C18	1.522(15)
N2–H2B	0.920	C19–C20	1.439(11)
N2–H2A	0.920		

Table S7. Hydrogen bonding geometry (Å, °) for **2**.

	$d(\text{D-H})/\text{Å}$	$d(\text{H}\cdots\text{A})/\text{Å}$	$d(\text{D}\cdots\text{A})/\text{Å}$	$\eta(\text{D-H}\cdots\text{A})/\text{°}$	symmetry operator
N1–H1 \cdots O3	0.880	1.840	2.578(7)	141.0	.
N2–H2A \cdots O1	0.920	1.830	2.703(7)	158.0	1+x, y, z
N2–H2B \cdots O4	0.920	1.860	2.696(7)	150.0	-1+x, y, z
N3–H3 \cdots O6	0.880	1.840	2.583(7)	140.0	.
C8–H8B \cdots O1	0.980	2.350	2.752(8)	104.0	.
C9–H9A \cdots Br1	0.990	2.850	3.720(7)	147.0	1-x, 1-y, -z
C9–H9B \cdots O3	0.990	2.430	3.125(8)	126.0	1-x, -y, -z
C11–H11A \cdots Br1	0.990	2.920	3.802(7)	149.0	.
C12–H12B \cdots O6	0.990	2.500	3.131(8)	122.0	1-x, -y, 1-z
C14–H14B \cdots O4	0.980	2.370	2.738(10)	101.0	.

Table S8. Selected bond lengths (Å) for **3**.

Cl4A-O42B	1.501(13)	C115-C116	1.437(5)
Cl4A-O43B	1.447(10)	C117-C119	1.327(4)
Cl4A-O43A	1.466(6)	C117-C118	1.476(5)
Cl4A-O41A	1.484(4)	C119-C120	1.436(5)
Cl4A-O42A	1.383(5)	O61-H61	0.820
Cl4A-O41B	1.479(14)	N21-C27	1.308(4)
Cl31-O31	1.483(3)	N21-C29	1.464(4)
Cl31-O32	1.501(3)	N22-C211	1.493(4)
Cl31-O33	1.451(3)	N22-C210	1.494(4)
O21-C21	1.212(4)	N23-C212	1.468(4)
O22-C22	1.374(4)	N23-C213	1.313(4)
O22-C21	1.393(4)	O71-C71	1.420(9)
O23-C25	1.259(4)	N21-H21	0.860
O24-C216	1.205(4)	N22-H22B	0.900
O25-C216	1.403(4)	N22-H22A	0.900
O25-C217	1.359(4)	N23-H23	0.860
O26-C220	1.271(4)	O71-H71	0.820
O11-C11	1.216(5)	N11-C19	1.453(5)
O12-C11	1.390(4)	N11-C17	1.316(5)
O12-C12	1.372(4)	N12-C110	1.488(4)
O13-C15	1.255(4)	N12-C111	1.492(4)
O14-C116	1.210(4)	N13-C112	1.464(5)
O15-C116	1.396(4)	N13-C113	1.307(4)
O15-C117	1.371(4)	N11-H11	0.860
O16-C120	1.274(4)	N12-H12B	0.900
O51-C51	1.431(7)	N12-H12A	0.900
O51-H51	0.820	N13-H13	0.860
O61-C61	1.362(9)	C21-C26	1.432(5)
C26-C27	1.433(5)	C22-C23	1.481(5)
C27-C28	1.500(5)	C22-C24	1.336(5)
C29-C210	1.514(5)	C24-C25	1.444(5)
C211-C212	1.518(5)	C25-C26	1.451(5)
C11-C16	1.423(5)	C16-C17	1.431(5)
C12-C13	1.476(5)	C217-C218	1.489(5)
C12-C14	1.329(5)	C17-C18	1.491(5)
C213-C214	1.498(5)	C217-C219	1.327(5)
C213-C215	1.436(5)	C19-C110	1.513(5)
C14-C15	1.440(5)	C219-C220	1.438(5)
C215-C220	1.441(5)	C113-C114	1.498(5)
C215-C216	1.448(5)	C113-C115	1.441(5)
C15-C16	1.443(5)	C111-C112	1.500(5)
C115-C120	1.440(4)		

Table S9. Hydrogen bonding geometry (Å, °) for **3**.

	$d(\text{D-H})/\text{Å}$	$d(\text{H}\cdots\text{A})/\text{Å}$	$d(\text{D}\cdots\text{A})/\text{Å}$	$\eta(\text{D-H}\cdots\text{A})/^\circ$	symmetry operator
N11-H11 \cdots O13	0.860	1.820	2.557(4)	142.0	.
N12-H12A \cdots Cl31	0.900	2.780	3.642(3)	161.0	.
N12-H12A \cdots O31	0.900	2.480	3.142(4)	130.0	.
N12-H12A \cdots O32	0.900	1.940	2.821(4)	164.0	.
N12-H12B \cdots O26	0.900	1.930	2.800(4)	161.0	.
N13-H13 \cdots O16	0.860	1.840	2.561(4)	141.0	.
N13-H13 \cdots O31	0.860	2.510	3.146(4)	131.0	.
N21-H21 \cdots O23	0.860	1.850	2.576(4)	141.0	.
N22-H22A \cdots O41A	0.900	2.040	2.840(5)	147.0	.
N22-H22A \cdots O14	0.900	2.500	3.143(4)	128.0	$3/2-x, -1/2+y, 3/2-z$
N22-H22B \cdots O16	0.900	1.850	2.740(3)	169.0	.
N23-H23 \cdots O26	0.860	1.870	2.586(4)	140.0	.
O61-H61 \cdots O11	0.820	2.040	2.857(5)	171.0	.
C111-H11C \cdots O61	0.970	2.590	3.475(5)	151.0	$1/2-x, 3/2+y, 3/2-z$
C13-H13D \cdots O21	0.960	2.510	3.416(6)	157.0	$3/2-x, -1/2+y, 3/2-z$
C14-H14 \cdots O21	0.930	2.570	3.396(4)	149.0	$3/2-x, -1/2+y, 3/2-z$
C18-H18A \cdots O51	0.960	2.550	3.487(5)	166.0	$x, 1+y, z$
C19-H19A \cdots O13	0.970	2.530	3.167(4)	123.0	$1-x, 2-y, 2-z$
C19-H19B \cdots O51	0.970	2.490	3.191(6)	129.0	$x, 1+y, z$
C210-H21A \cdots O31	0.970	2.590	3.400(5)	141.0	.
C210-H21A \cdots O23	0.970	2.560	3.147(4)	119.0	$1-x, 2-y, 1-z$
C210-H21B \cdots O15	0.970	2.370	3.239(4)	150.0	$3/2-x, -1/2+y, 3/2-z$
C211-H21C \cdots O15	0.970	2.540	3.372(4)	144.0	$3/2-x, -1/2+y, 3/2-z$
C211-H21D \cdots O31	0.970	2.600	3.400(4)	140.0	.
C214-H21I \cdots O24	0.960	2.400	2.800(4)	104.0	.
C214-H21J \cdots O24	0.960	2.050	2.800(4)	134.0	.
C23-H23D \cdots O24	0.960	2.470	3.368(5)	155.0	$-1/2+x, 5/2-y, -1/2+z$
C23-H23E \cdots O51	0.960	2.540	3.455(6)	160.0	$1/2+x, 3/2-y, -1/2+z$
C24-H24 \cdots O24	0.930	2.580	3.384(4)	145.0	$-1/2+x, 5/2-y, -1/2+z$
C28-H28B \cdots O21	0.960	2.370	2.794(4)	106.0	.
C28-H28D \cdots O21	0.960	2.060	2.794(4)	132.0	.
C119-H119 \cdots O41A	0.930	2.370	3.300(5)	173.0	.
C219-H219 \cdots O61	0.930	2.440	3.325(5)	158.0	$1/2-x, 3/2+y, 3/2-z$

NMR studies

One-dimensional ^1H spectra were recorded with Bruker AV-600 and Bruker AV-300 Fourier-transform spectrometer operating at 600.13 (and 300.13) MHz, 74.45 MHz and 121.46 MHz for ^1H . Spectra were recorded in DMSO-*d*₆ at 302 K containing SiMe₄ as an internal standard. **L**: ^1H NMR (300 MHz, DMSO) δ 13.68 (s, 2H), 5.62 (d, J = 0.8 Hz, 2H), 3.55 (dd, J = 10.8, 5.5 Hz, 4H), 2.83 (d, J = 5.5 Hz, 4H), 2.55 (s, 6H), 2.24 (s, 1H), 2.06 (d, J = 0.6 Hz, 6H). **1a**: ^1H NMR (300 MHz, DMSO) δ 13.76 (s, 2H), 8.67 (s, 2H), 5.74 (d, J = 0.7 Hz, 2H), 3.84 (q, J = 6.1 Hz, 4H), 3.30 (d, J = 13.0 Hz, 4H), 2.60 (s, 6H), 2.09 (s, 6H). **1b**: ^1H NMR (600 MHz, DMSO) δ 13.76 (s, 2H), 8.69 (s, 2H), 5.74 (s, 2H), 3.83 (d, J = 5.4 Hz, 4H), 2.60 (s, 6H), 2.09 (s, 6H).

The results of ^1H NMR investigations (DMSO-*d*₆) of free **L** and complexes are presented in Figure S9. In the spectrum of **L**, two most interesting features are the chemical shifts of proton in central and peripheral amino groups. The position of central amino proton (N2–H2 proton; 2.23 ppm) reveals that this group is not involved in strong interactions with environment, whereas the position of peripheral amino hydrogen atoms (13.68 ppm) complies with the structurally determined involvement of these groups in strong intramolecular N–H \cdots O hydrogen bonding. When comparing the ^1H NMR spectrum of **L** in CDCl₃, same protons are shifted downfield (14.18 ppm), and the central amino proton is shifted upfield to 1.34 ppm, which could be tentatively ascribed to solvent effect. Engagement of peripheral amino protons in strong hydrogen bonding is additionally confirmed by the position and shape of the –C9–H2 signal. This signal is broad triplet (2.82 ppm in DMSO-*d*₆ and 3.02 ppm in CDCl₃) indicating the main influence of neighbouring –C10–H2 group and weak interactions of C9 with an amino proton. Signal of C10 methylene group is found as a quartet at 3.48 ppm with low J values. Singlets corresponding to methyl groups' protons are found at 2.06 ppm (C4) and 2.54 ppm (C8).

Spectra of supramolecular complexes in DMSO-*d*₆ confirmed protonation of central amino group, with corresponding singlet shifted from 2.23 ppm in **L** to \approx 8.69 ppm in complexes, whereas other signals corresponding to methyl- and methylene groups show much smaller shifts. Also, the signal corresponding to peripheral amino groups can be observed at 13.74 ppm. Altogether, ^1H NMR spectra revealed that, despite their different solid-state structures and host-guest interactions, the investigated complexes have almost identical spectrum in DMSO-*d*₆ solution.

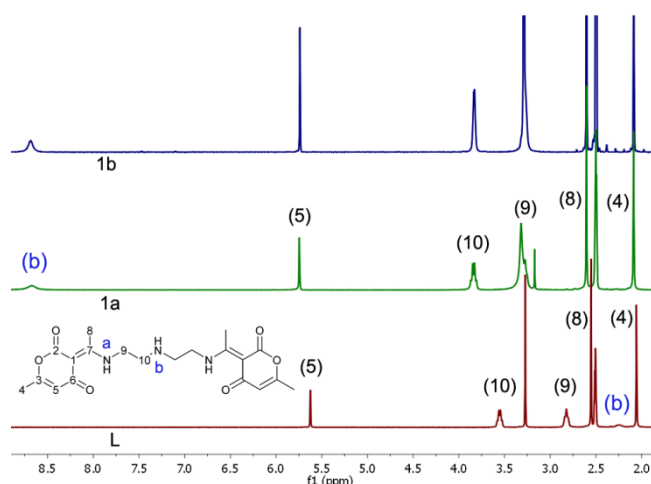


Figure S9. ^1H NMR spectra of apohost **L** (red) and complexes **1a** (green) and **1b** (blue).

References

- [1] CrysAlisPro, Oxford Diffraction Ltd., Version 1.171.33.66, 2010.
- [2] G. M. Sheldrick, *SHELXS*, Program for the Solution of Crystal Structures, University of Göttingen, Germany, 1997.
- [3] (a) G. M. Sheldrick, *Acta Cryst. A*, 2008, **64**, 112-122. (b) G. M. Sheldrick, *SHELXS-2014*, Program for Crystal Structure Solution, University of Göttingen, 2014; (c) G. M. Sheldrick, *SHELXL*, Version 2014/7, Program for Crystal Structure Refinement, University of Göttingen, 2014.
- [4] L. J. Farrugia, *J. Appl. Crystallogr.*, **1999**, *32*, 837–838.
- [5] A. L. Spek, *J. Appl. Cryst.*, **2003**, *36*, 7–13.
- [6] L. J. Farrugia, *J. Appl. Crystallogr.* **1997**, *30*, 565.
- [7] J. Bruno, J. C. Cole, P. R. Edgington, M. K. Kessler, C. F. Macrae, P. McCabe, J. Pearson, R. Taylor, *Acta Crystallogr.*, **2002**, *B58*, 389-397.
- [8] S.K. Wolff, D.J. Grimwood, J.J. McKinnon, M.J. Turner, D. Jayatilaka, M.A. Spackman, CrystalExplorer (Version 3.1), , University of Western Australia, 2012.